Endothelial Wnt/β-catenin signaling reduces immune cell infiltration in multiple sclerosis

Justin E. Lengfeld[a,1], Sarah E. Lutz[b,1,2], Julian R. Smith[b], Claudiu Diaconu[b], Cameron Scott[a], Sigal B. Kofman[c], Claire Choi[b], Craig M. Walsh[d], Cedric S. Raine[e], Ilir Agalliu[f], and Dritan Agalliu[a,b,g,h,2]

[a]Department of Developmental and Cell Biology, University of California, Irvine, CA 92697; [b]Department of Neurology, Columbia University Medical Center, New York, NY 10032; [c]Department of Medicine, Columbia University Medical Center, New York, NY 10032; [d]Department of Molecular Biology and Biochemistry, University of California, Irvine, CA 92697; [e]Department of Pathology, Albert Einstein College of Medicine, Bronx, NY 10461; [f]Department of Epidemiology and Population Health, Albert Einstein College of Medicine, Bronx, NY 10461; [g]Department of Pathology and Cell Biology, Columbia University Medical Center, New York, NY 10032; and [h]Department of Pharmacology, Columbia University Medical Center, New York, NY 10032

Edited by Lawrence Steinman, Stanford University School of Medicine, Stanford, CA, and approved December 29, 2016 (received for review June 20, 2016)

Disruption of the blood–brain barrier (BBB) is a defining and early feature of multiple sclerosis (MS) that directly damages the central nervous system (CNS), promotes immune cell infiltration, and influences clinical outcomes. There is an urgent need for new therapies to protect and restore BBB function, either by strengthening endothelial tight junctions or suppressing endothelial vesicular transcytosis. Although wingless integrated MMTV (Wnt)/β-catenin signaling plays an essential role in BBB formation and maintenance in healthy CNS, its role in BBB repair in neurologic diseases such as MS remains unclear. Using a Wnt/β-catenin reporter mouse and several downstream targets, we demonstrate that the Wnt/β-catenin pathway is up-regulated in CNS endothelial cells in both human MS and the mouse model experimental autoimmune encephalomyelitis (EAE). Increased Wnt/β-catenin activity in CNS blood vessels during EAE progression correlates with up-regulation of neuronal Wnt3 expression, as well as breakdown of endothelial cell junctions. Genetic inhibition of the Wnt/β-catenin pathway in CNS endothelium before disease onset exacerbates the clinical presentation of EAE, $CD4^+$ T-cell infiltration into the CNS, and demyelination by increasing expression of vascular cell adhesion molecule-1 and the transcytosis protein Caveolin-1 and promoting endothelial transcytosis. However, Wnt signaling attenuation does not affect the progressive degradation of tight junction proteins or paracellular BBB leakage. These results suggest that reactivation of Wnt/β-catenin signaling in CNS vessels during EAE/MS partially restores functional BBB integrity and limits immune cell infiltration into the CNS.

blood–brain barrier | endothelial cell | Wnt/β-catenin signaling | MS | EAE

In both multiple sclerosis (MS) and its animal model experimental autoimmune encephalomyelitis (EAE), leukocytes infiltrate the central nervous system (CNS) across a damaged blood–brain barrier (BBB) to mediate myelin destruction and neuronal damage (1). BBB breakdown is a contributing factor to the pathogenesis of both MS and EAE (2–4). Structural and functional BBB degradation precedes lesion development in both MS and EAE (5–9), and focal BBB abnormalities correlate with clinical exacerbations in the relapsing-remitting form of MS (10). Moreover, BBB leakage precedes the entry of T cells and monocytes into the brain parenchyma (7, 11) and coincides with early infiltration of neutrophils before the onset of EAE (12). Although the severity of barrier leakage decreases over time for most relapsing-remitting MS lesions, as assessed by gadolinium-enhancing magnetic resonance imaging (7, 13–15), whether BBB recovery is an active process and, if so, which pathways mediate its repair, remain unclear.

The BBB achieves its highly selective permeability through the presence of (*i*) tight junctions (TJs) that prevent paracellular diffusion of small molecules and immune cells between endothelial cells (ECs), (*ii*) very few endocytotic vesicles that restrict movement of large molecules through the transcellular pathway, and (*iii*) transporters that shuttle select nutrients between the blood and the brain (3). The junctional transmembrane proteins Claudin-3, -5, and -12 and Occludin are expressed at the BBB and form paracellular pores via extracellular homotypic interactions, with Claudin-5 being essential for barrier function (16–18). Although sparse, endocytotic caveolae in the CNS endothelium provide an essential route for receptor-mediated transcytosis (19, 20). This process requires Caveolin-1 (Cav-1), a transmembrane protein expressed at low levels within CNS blood vessels (21–23). Cav-1 levels are known to increase during BBB breakdown following ischemic stroke, when enhanced transcytosis initiates BBB dysfunction (24, 25). Finally, healthy BBB vasculature has low levels of leukocyte adhesion molecules, such as vascular cell adhesion molecule (VCAM)-1 and intercellular adhesion molecules (ICAMs)-1 and -2, which are up-regulated on CNS vessels during EAE/MS to promote T-cell trafficking into the parenchyma (26–29). Blockade of VCAM-1 interactions with its cognate lymphocyte ligand integrin α4 reduces the clinical severity of EAE (30) and is the basis for MS-modifying therapy with natalizumab (31).

These unique properties of the BBB are formed and maintained by the wingless integrated MMTV (Wnt)/β-catenin pathway. Loss of Wnt/β-catenin signaling in developing blood vessels disrupts CNS angiogenesis and prevents BBB formation (32–34). Although Wnt signaling is reduced in CNS blood vessels once the barrier is fully formed, this pathway is essential to maintain barrier properties in the adult CNS (35). Activation of Wnt/β-catenin signaling has been reported in some neuroinflammatory

Significance

Endothelial cells (ECs) in the CNS form a unique blood–brain barrier (BBB) that is broken down in multiple sclerosis (MS). New therapies are sorely needed to restore BBB function in this disease. The wingless integrated MMTV (Wnt)/β-catenin pathway, which is essential for barrier formation, is activated in CNS ECs in MS and the animal model experimental autoimmune encephalomyelitis. When this pathway is inhibited in ECs before disease onset, mice develop more severe disease, with more immune cells entering the CNS owing to increased levels of proteins that promote interactions of immune cells with blood vessels and transport across vessels. Our findings suggest that pharmacologic enhancement of Wnt signaling may be helpful to limit BBB damage and CNS immune cell infiltration in MS.

Author contributions: J.E.L., S.E.L., and D.A. designed research; J.E.L., S.E.L., J.R.S., C.D., C.S., S.B.K., C.C., and D.A. performed research; C.M.W. and C.S.R. contributed new reagents/analytic tools; J.E.L., S.E.L., J.R.S., C.D., C.S., S.B.K., C.C., I.A., and D.A. analyzed data; and J.E.L., S.E.L., and D.A. wrote the paper.

The authors declare no conflict of interest.

This article is a PNAS Direct Submission.

[1]J.E.L. and S.E.L. contributed equally to this work.

[2]To whom correspondence may be addressed. Email: da191@cumc.columbia.edu or sl4151@cumc.columbia.edu.

This article contains supporting information online at www.pnas.org/lookup/suppl/doi:10.1073/pnas.1609905114/-/DCSupplemental.

diseases. Disruption of endothelial adherens junctions (AJs) within active MS lesions releases β-catenin from the plasma membrane (36) and results in transcriptional activity (37, 38). Moreover, Wnt-3a and -5a are expressed in the dorsal spinal cord during EAE (39), and both T-cell factor 4 (Tcf4) and adenomatosis polyposis coli downregulated 1 (Apcdd1), a transcriptional downstream Wnt target (40, 41), are expressed in subsets of oligodendrocytes in active MS/EAE lesions (42–45). Despite previous studies demonstrating up-regulation of Wnt signaling components in MS/EAE lesions, a role for this pathway in the pathogenesis of neuroinflammatory diseases remains unclear, because its effect depends on the specific cell type in which the pathway is active. Activation in oligodendrocytes suppresses their differentiation and myelination, and may be detrimental for repair processes within the CNS (44, 46); however, Wnt signaling in dendritic cells suppresses neuroinflammation and ameliorates EAE by diminishing Th1/Th17 immune responses (47).

Despite an essential role for Wnt/β-catenin signaling in BBB formation and maintenance, and its reported activity in MS/EAE lesions, whether this pathway plays any role in barrier protection or repair during neuroinflammation is not clear. We have examined the activation of Wnt/β-catenin signaling in CNS ECs during EAE progression, using both a *TCF/LEF1*::H2B-eGFP Wnt reporter mouse (48) and several downstream targets. We found that Wnt/β-catenin activity is increased in CNS blood vessels during EAE, and coincides with up-regulation of Wnt-3 and -5a expression, as well as progressive destruction of endothelial junctions. Furthermore, inducible inhibition of this pathway in ECs results in clinically exacerbated EAE, increased $CD4^+$ T-cell infiltration into the CNS, enhanced expression of both VCAM-1 and Cav-1, and an increased rate of endothelial transcytosis. Thus, our findings reveal a previously unknown role for endogenous Wnt/β-catenin signaling in partially reversing the BBB disruption that occurs during MS/EAE and, more importantly, establish a crucial role for this pathway in reducing immune cell infiltration during neuroinflammation.

Results

The Wnt/β-Catenin Pathway Is Activated in CNS ECs During EAE. To investigate whether the Wnt/β-catenin pathway is activated during EAE, we used *TCF/LEF1*::H2B-eGFP Wnt reporter transgenic mice that express a fusion of green fluorescent protein (eGFP) with histone H2B protein under the control of the TCF/LEF1 response element, a β-catenin transcriptional target (48) (Fig. 1*A*). These mice allow visualization of Wnt/β-catenin pathway activation because of their nuclear eGFP expression. We first confirmed that this strain accurately reports Wnt activity in CNS blood vessels during embryonic development. We quantified the percentage of $eGFP^+$ blood vessel nuclei in thoracic and lumbar neural tubes at three stages of embryonic development, and found that Wnt signaling decreases in CNS blood vessels from embryonic day (E) 11.5 (~80–90%) to E18.5 (~10–30%) (*SI Appendix*, Fig. S1), consistent with previous studies (32–34).

We then immunized *TCF/LEF1*::H2B-eGFP reporter mice with myelin oligodendrocyte glycoprotein peptide $(MOG)_{35–55}$

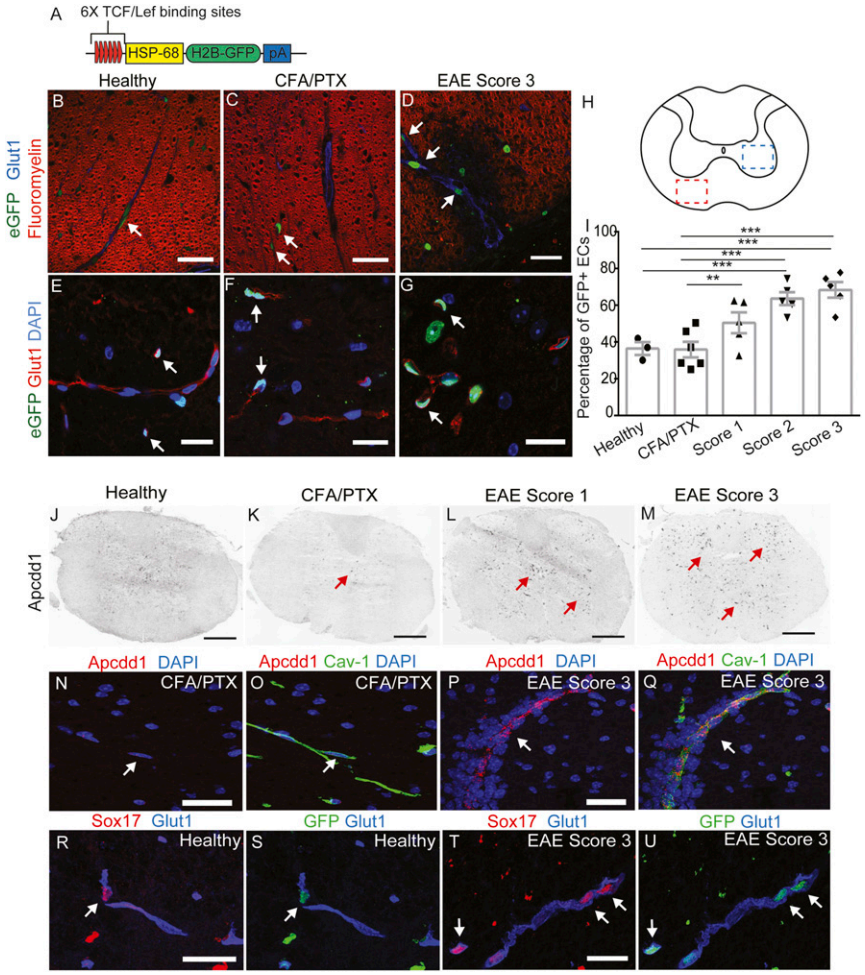

Fig. 1. The Wnt/β-catenin pathway is up-regulated in thoracic spinal cord ECs during EAE. (*A*) Diagram of the *TCF/LEF1*::H2B-eGFP Wnt reporter transgene. (*B–H*) Immunofluorescence for eGFP (green), fluoromyelin (myelin; red), and Glut-1 (blood vessels; blue) in the white matter of thoracic spinal cords from the Wnt reporter strain. Wnt activity (eGFP immunofluorescence) is increased in white matter thoracic spinal cord ECs (*H*, red square; *B–D*, white arrows) during EAE progression. Wnt reporter activity is also increased in ECs in the gray matter of thoracic spinal cords during EAE progression (*H*, blue square; *E–G*, white arrows). Glut-1 (red) labels blood vessels, and DAPI indicates nuclei. (*I*) Quantification of Wnt reporter activity in thoracic spinal cord ECs during EAE progression. Healthy, $n = 3$; CFA/PTX, $n = 6$; EAE score 1–3, $n = 5$. $^{**}P < 0.01$, $^{***}P < 0.001$, mixed-effects ANOVA. (*J–M*) In situ hybridization for *Apcdd1* during progression of EAE in thoracic spinal cords. Apccd1 mRNA levels are increased at EAE scores 1 and 3 (red arrows). (*N–Q*) In situ hybridization for *Apcdd1* (red) combined with immunofluorescence for Cav-1 (blood vessel marker; green) in CFA/PTX controls and EAE score 3. Apcdd1 mRNA is up-regulated during EAE progression and colocalizes with Cav-1. (*R–U*) Immunofluorescence for Sox17 (red), eGFP (green), and Glut-1 (blue) in healthy and EAE score 3 thoracic spinal cords. Sox17 is up-regulated in the vasculature during EAE, and colocalizes with eGFP in Wnt reporter mice (white arrows). (Scale bars: 20 μm; 200 μm in *J* and *K*).

plus complete Freund's adjuvant (CFA) emulsion combined with i.v. administration of *Bordetella pertussis* toxin (49), and quantified the percentage of eGFP$^+$ ECs in both gray and white matter thoracic and lumbar spinal cords during disease progression. We observed increased Wnt reporter activity in blood vessels located in both demyelinated white matter lesions and in the gray matter of the spinal cord from mice with EAE (Fig. 1 *B–I* and *SI Appendix*, Fig. S2 *A–H*). The fraction of eGFP$^+$ EC nuclei in both thoracic and lumbar spinal cords increased significantly during peak EAE clinical scores (~65–70%; scores 2 and 3) compared with either healthy mice (~35–40%) or CFA plus *B. pertussis* toxin (CFA/PTx) control mice (~35–40%) (Fig. 1*I* and *SI Appendix*, Fig. S2*H*; $^*P < 0.05$, $^{**}P < 0.01$, $^{***}P < 0.001$, mixed-effects ANOVA).

We next examined the expression of two downstream Wnt/β-catenin pathway target genes, *Apcdd1* and sex determining region Y-box 17 (*Sox17*) (40, 50), in spinal cords during EAE. In both vascular and nonvascular cells, expression of *Apcdd1* mRNA was highly increased by EAE scores 1 and 3 using in situ hybridization with an antisense DIG-labeled probe (Fig. 1 *J–M* and *SI Appendix*, Fig. S2 *I–P*). We performed fluorescence in situ hybridization for *Apcdd1* mRNA combined with immunofluorescence for Cav-1, and confirmed high expression of *Apcdd1* in CNS vasculature by EAE score 3 (Fig. 1 *N–Q*), similar to its vascular expression during development (51). Sox17 expression also was significantly increased in CNS venules and capillaries during EAE progression, and colocalized with eGFP in ECs of the Wnt reporter spinal cords (Fig. 1 *R–U*). Taken together, these data demonstrate that the Wnt/β-catenin pathway is reactivated in CNS blood vessels during EAE progression.

***Wnt3* Is Up-Regulated in Neurons During EAE.** To determine which Wnt ligands might signal to CNS ECs to activate the pathway during EAE, we screened several Wnt ligands and Norrin by in situ hybridization using EAE spinal cord tissue (*SI Appendix*, Table S1). *Wnt-3* and *Wnt-5a* mRNAs showed increased expression in both the thoracic and lumbar spinal cord with disease progression (Fig. 2 *A–P* and *SI Appendix*, Fig. S3 and Table S1). Transcripts for *Wnt-3*, a canonical Wnt/β-catenin pathway activator (52), were predominantly up-regulated in the gray matter of the spinal cord during EAE (Fig. 2 *A–P*), where the majority of eGFP$^+$ ECs were found in Wnt reporter mice as well. *Wnt-3* mRNA was not colocalized with the GFAP$^+$ reactive astrocytes, but was colocalized with the NeuN$^+$ neurons (Fig. 2 *Q–T*), indicating that *Wnt-3* mRNA is up-regulated in neurons during EAE progression. *Wnt-5a* mRNA, a ligand that typically acts through noncanonical Wnt signaling but can activate the Wnt/β-catenin pathway (53), also showed increased gray matter expression during EAE progression (*SI Appendix*, Fig. S3 *A–D* and Table S1). In contrast, the *Wnt-7a* and *-7b* ligands, which promote CNS angiogenesis and BBB development (32–34), were either at low levels or absent during EAE (*SI Appendix*, Fig. S3 *E–H* and Table S1). Thus, the *Wnt-3* and *-5a* ligands are expressed concomitantly with increased Wnt signaling activity in CNS blood vessels during EAE, and may signal to CNS ECs to activate the pathway.

Progressive Destruction of EC Junctions Correlates with Wnt Signaling Activation in CNS Blood Vessels During EAE. An alternative mechanism of Wnt/β-catenin pathway activation relies on the release of β-catenin, which has a structural role in AJs between cells (54), when cell junctions are destroyed (37, 55, 56). Because the breakdown of AJs and TJs occurs in active MS lesions (57) and in MOG$_{35–55}$ EAE (58), we collected whole spinal cord lysates from C57BL/6J mice with EAE and performed Western blot analyses for various AJ and TJ components, to correlate their degradation with Wnt signaling activation. Several TJ components, including Claudin-5, Occludin, and ZO-1, showed markedly decreased protein levels during peak EAE (*SI Appendix*, Fig. S4 *A–D*). The AJ protein Cadherin-5 (VE-cadherin) also was significantly decreased during peak EAE (*SI Appendix*, Fig. S4*E*); however,

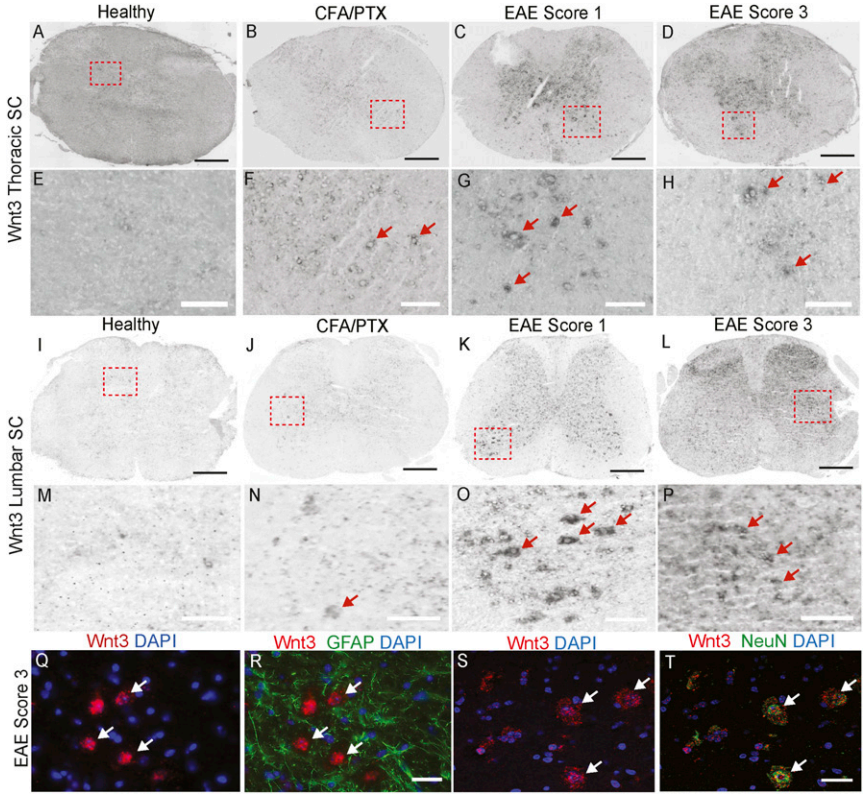

Fig. 2. *Wnt-3* is up-regulated in neurons during EAE progression. (*A–P*) In situ hybridization for *Wnt3* in thoracic and lumbar spinal cords from healthy CFA/PTX controls as well as EAE score 1 and 3 mice. Wnt3 mRNA is highly up-regulated at EAE scores 1 and 3 (*G*, *H*, *O*, and *P*, red arrows). (*Q–T*) Fluorescence in situ hybridization for *Wnt3* combined with immunofluorescence for GFAP (astrocytic marker) and NeuN (neuronal marker). *Wnt3* is not expressed in reactive GFAP$^+$ astrocytes, but is highly up-regulated in NeuN$^+$ neurons at EAE score 3 (*S* and *T*, white arrows). (Scale bars: 200 μm in *A–D* and *I–L*; 20 μm in *E–H* and *M–T*.)

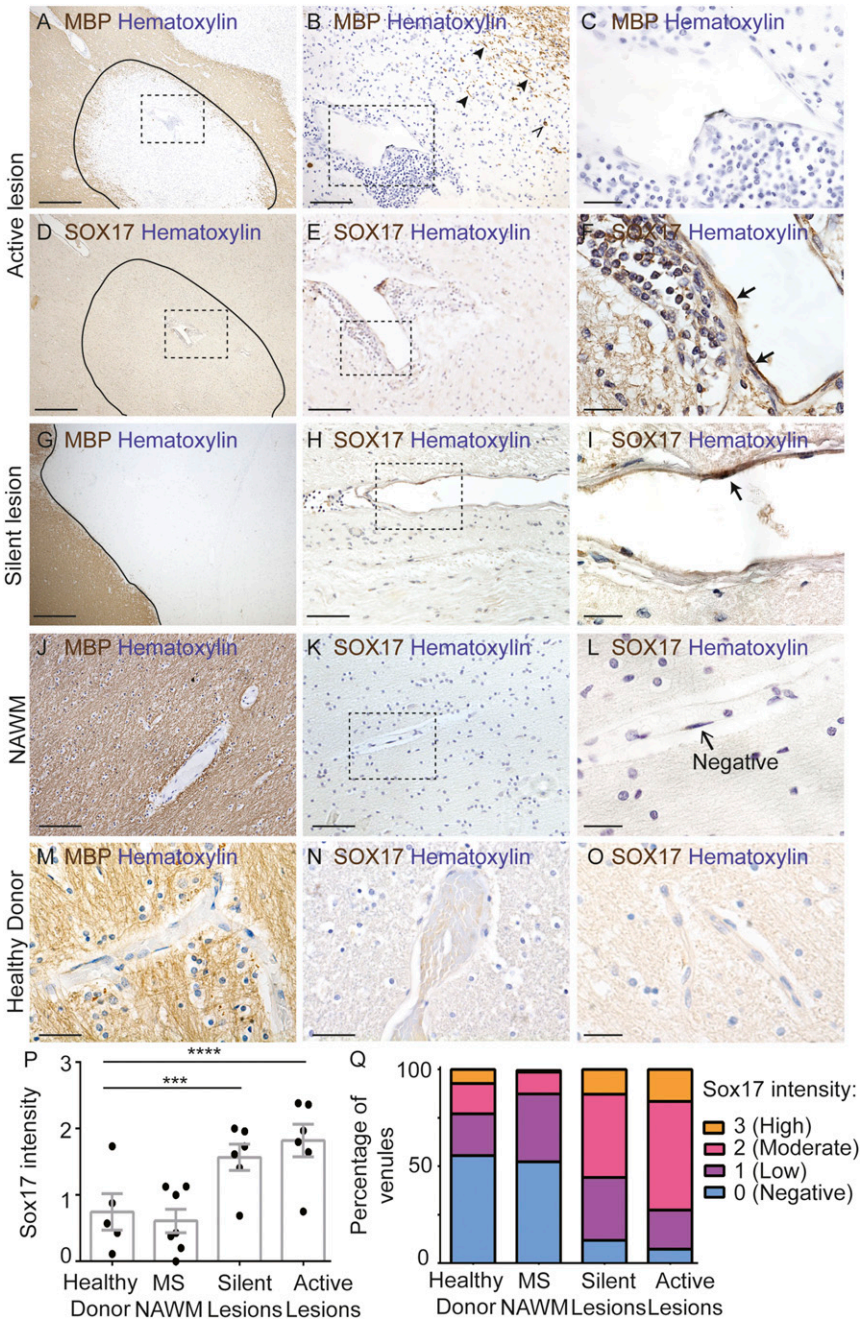

Fig. 3. Increased endothelial SOX17 expression in active multiple sclerosis lesions. (*A–C*) Immunohistochemistry for myelin basic protein (MBP; brown) and hematoxylin (blue) within an active lesion. (*A*) The lesion edge is indicated by a solid black line. (*B*) Higher-magnification view of the boxed region in *A* showing few regions with intact myelin (arrowheads) and some phagocytic cells with intracellular myelin (open arrowhead). (*C*) Higher-magnification view of the boxed region in *B* illustrating extensive perivascular infiltrate around an inflamed venule. (*D–F*) Immunohistochemistry for SOX17 (brown) and hematoxylin (blue) in adjacent serial sections from the same active lesion depicted in *A–C*. (*F*) ECs in the inflamed venule exhibit intense SOX17 immunoreactivity (black arrows). SOX17 is also expressed in some leukocytes. (*G*) MBP immunohistochemistry in a chronic silent lesion (hematoxylin; blue). The lesion edge is delineated by a solid black line. (*H*) SOX17 immunohistochemistry in the same chronic silent lesion (section adjacent to *G*). (*I*) Representative images of venular ECs with high and low nuclear SOX17 expression. (*J*) MBP immunohistochemistry in normal-appearing white matter (NAWM) from the same case as *A–F*. NAWM has robust MBP expression. (*K* and *L*) SOX17 immunohistochemistry in NAWM from the same case as in *A–F*. In NAWM, endothelial SOX17 expression is either low or absent. (*M*) Robust MBP expression in white matter from a nonneurologic control. (*N* and *O*) Minimal SOX17 expression in white matter from a nonneurologic disease control. (*P*) Graph of SOX17 intensity in venule ECs from human nonneurologic disease control, MS NAWM, silent and active MS lesions. SOX17 intensity is significantly increased in active lesions (***$P < 0.001$) and in silent lesions (**$P < 0.01$); mixed-effects ANOVA compared with nonneurologic disease controls. (*Q*) Stacked bar graph of SOX17 intensity distribution among groups ($n = 6$ active lesions, $n = 6$ silent lesions, $n = 7$ NAWM regions, $n = 5$ nonneurological disease controls) from 12 MS patients and 5 non-MS donors. (Scale bars: 500 μm in *A*, *D*, and *G*; 100 μm in *E*, *H*, *J*, *K*, *M*, *N*, and *O*; 66 μm in *B*; 20 μm in *C*, *F*, *I*, and *L*.)

α- and β-catenin levels showed no significant reduction during EAE progression (*SI Appendix*, Fig. S4 *E–G*). These findings confirm that the degradation of AJ and TJ structural components peaks at EAE score 3, when Wnt signaling is most active in CNS blood vessels, and suggest that putative β-catenin release from degraded endothelial AJs could promote the transcription of downstream Wnt/β-catenin pathway targets in CNS blood vessels.

Activation of the Wnt/β-Catenin Pathway Occurs in Blood Vessels of MS Lesions. We next asked whether activation of canonical Wnt/β-catenin signaling occurs in the vasculature of MS lesions. We assessed SOX17 expression by immunohistochemistry in formalin-fixed, paraffin-embedded brain sections from 12 MS patients and 5 nonneurologic disease controls (*SI Appendix*, Table S2). Active lesions exhibited extensive demyelination and perivascular leukocyte infiltration (Fig. 3 *A–C*). The majority (93%) of venules in active lesions contained ECs with varying degrees of SOX17 expression (Fig. 3 *D–F*, *P*, and *Q*). Approximately 73% of venules showed moderate/high SOX17 expression, and 27% showed negative/low SOX17 expression (Fig. 3 *P* and *Q*). Furthermore, in chronic silent lesions, defined by demyelination and minimal perivascular inflammation (Fig. 3*G*), SOX17 expression was present in the majority (88%) of venules; ∼56% exhibited moderate/high and 44% negative/low SOX17 expression (Fig. 3 *H*, *I*, *P*, and *Q*). In contrast, SOX17 expression was low or absent in normal-appearing white matter from MS patients (Fig. 3 *J–L*, *P*, and *Q*; 12% moderate/high expression, 87% negative/low expression) and in white matter from five controls (Fig. 3 *M–Q*; 23% moderate/high expression, 77% negative/low expression). The mean SOX17 intensity was significantly higher in active lesions (mean, 1.8; $P < 0.001$) and in silent lesions (mean, 1.6; $P < 0.01$) compared with nonneurologic disease

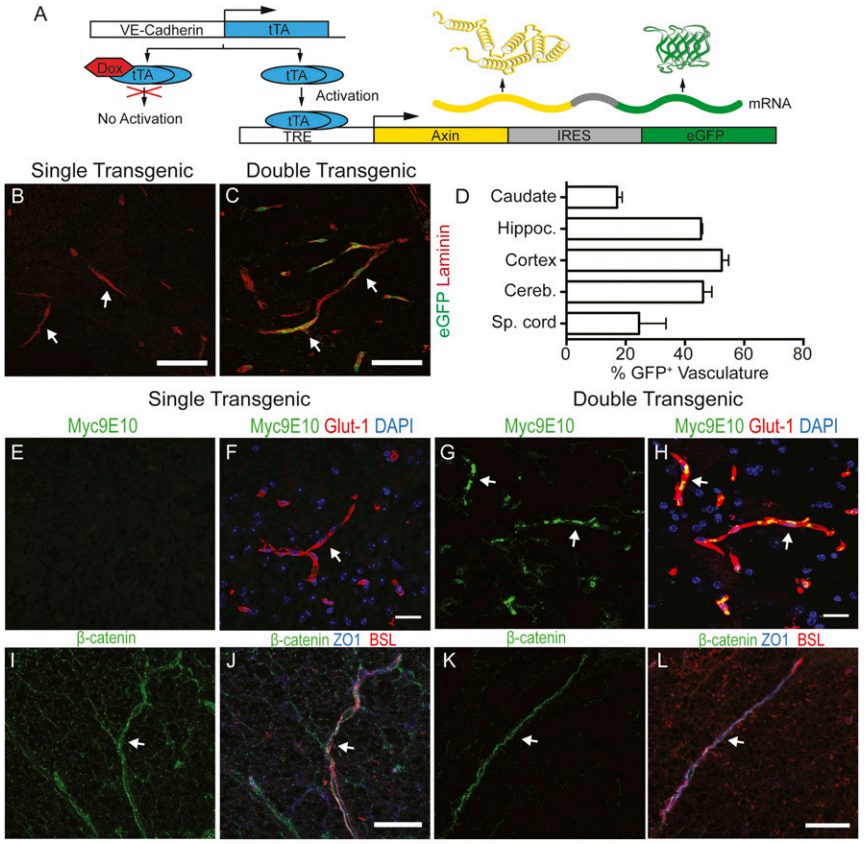

Fig. 4. Genetic inhibition of Wnt/β-catenin signaling in CNS ECs does not affect endothelial AJ and TJ formation in healthy mice. (*A*) Diagram of Axin overexpression in CNS ECs by the Tet_{OFF} binary system. (*B* and *C*) Immunofluorescence for eGFP (green) and Laminin (red) in adult spinal cords from singly transgenic (sTg; TRE-Axin-IRES-eGFP$^{+/-}$) or doubly transgenic (dTg; VE-Cadherin tTA$^{+/-}$; TRE-Axin-IRES-eGFP$^{+/-}$) healthy mice at 60 d after removal of doxycycline-containing food. eGFP in blood vessels (Laminin, red) indicates expression of Axin and eGFP in dTg mice, but not in sTg mice (white arrows). (*D*) Graph showing the fraction of eGFP^{+} ECs in various CNS regions from dTg healthy mice ($n = 3$). (*E–H*) Immunofluorescence for c-Myc (Myc9E10; green), Glut-1 (blood vessel marker; red), and DAPI (nuclei; blue) in sTg mice (*E* and *F*) and dTg mice (*G* and *H*). Myc colocalizes with the vascular marker Glut-1 in dTg mice (*G* and *H*; white arrows). (*I* and *J*) Immunofluorescence for β-catenin (green), ZO-1 (blue), and BSL (blood vessel marker; red) in sTg and dTg mice. dTg mice have intact junctional β-catenin expression in ECs that colocalizes with the TJ protein ZO-1. (Scale bars: 20 μm.)

white matter (mean, 0.74) (Fig. 3*P*). These findings indicate that SOX17, a downstream target of the canonical Wnt/β-catenin pathway, is reactivated in brain ECs in human MS lesions, similar to mouse spinal cords with EAE.

We also examined expression of APCDD1 mRNA and protein in fresh frozen tissues from six MS patients and five non-neurologic disease controls (*SI Appendix*, Table S2). APCDD1 protein was present at low levels in lysates from white matter of control patients with nonneurologic disease, as well as from normal-appearing white matter from MS patients; however, APCDD1 protein levels were up-regulated in the majority of lysates from MS lesions (*SI Appendix*, Fig. S5 *A* and *B*). We next examined the expression of *APCDD1* mRNA by in situ hybridization in tissue sections and compared it with *CLAUDIN5* mRNA. White matter from healthy nonneurologic controls and normal-appearing white matter from MS patients had either absent or low *APCDD1* mRNA expression in blood vessels (*SI Appendix*, Fig. S5 *C–F*, *G*, *H*, *K*, and *L* and Table S3); however, *APCDD1* mRNA was highly up-regulated in the majority of MS lesions, and two of the six MS patients had either low or absent *APCDD1* mRNA expression (*SI Appendix*, Fig. S5 *I*, *J*, *M*, and *N* and Table S3). *APCDD1* mRNA was expressed predominantly in endothelial cells in a pattern similar to that seen with *CLAUDIN5*; however, there was some nonvascular APCDD1 expression in MS lesions. Therefore, the up-regulation of both SOX17 and APCDD1 expression in MS lesions confirms that the canonical Wnt/β-catenin pathway is reactivated in brain ECs in MS lesions.

EC-Specific Inhibition of the Wnt/β-Catenin Pathway Exacerbates EAE. To establish a role for increased Wnt/β-catenin pathway activity in ECs during EAE, we crossed a VE-Cadherin::tTA transgenic strain (59) with a TRE-Axix-IRES-eGFP strain (60) to generate doubly transgenic (dTg) mice that overexpress the Wnt inhibitor Axin and eGFP specifically in ECs, in a doxycycline-regulated manner (Fig. 4*A*). We fed the dTg mice with doxycycline during gestation to repress transgene expression in ECs, thereby allowing normal development of the BBB. We then removed doxycycline at birth and assessed the expression of c-myc–tagged Axin and eGFP in blood vessels of dTg and singly transgenic TRE-Axin-IRES-eGFP (sTg) mice around postnatal day (P) 60. eGFP was expressed in ∼20–60% of CNS blood vessels depending on CNS region (∼25% of blood vessels are eGFP^{+} in the spinal cord; Fig. 4 *A–D*). Moreover, we detected expression of myc-tagged Axin protein in spinal cord blood vessels in dTg mice (Fig. 4 *G* and *H*). In contrast, neither VE-Cadherin::tTA nor TRE-Axin-IRES-eGFP sTg mice showed eGFP and c-Myc expression in CNS blood vessels (Fig. 4 *B*, *E*, and *F*). Despite Axin overexpression in CNS ECs, the levels of various AJ and TJ proteins, as well as subcellular localization of β-catenin and ZO-1, were normal in blood vessels from healthy mice of both genotypes, suggesting no defects in endothelial junctions (Fig. 4 *I–L* and *SI Appendix*, Fig. S6 *A–E*). Expression of other BBB components, including Cav-1, Cavin-2, and Glut-1, was similar in sTg and dTg healthy mice (*SI Appendix*, Fig. S6 *F–H*).

We induced EAE in both dTg and sTg littermate controls between P60 and P75 and collected spinal cords for evaluation at day 15 postinduction (Fig. 5*A*). We noticed that high proportions of both sTg and dTg mice did not exhibit any clinical signs of EAE or had low clinical scores (Fig. 5 *B–D*). This is likely due to some residual antibiotic accumulated in the bone that could affect disease outcome, because minocycline suppresses EAE (61), reducing the expression of LFA-1 in CD4^{+} and CD8^{+} T cells and immune cell infiltration into the CNS (62). Nonetheless, the clinical scores for all mice were significantly higher in dTg mice compared with sTg mice from 12 to 15 d postinduction, including those that did not exhibit any signs (score 0), were sick (variable scores), or died during disease (assigned a score of 6.0 from the day of death) (sTg, $n = 38$; dTg, $n = 32$; $^{*}P < 0.05$, two-way

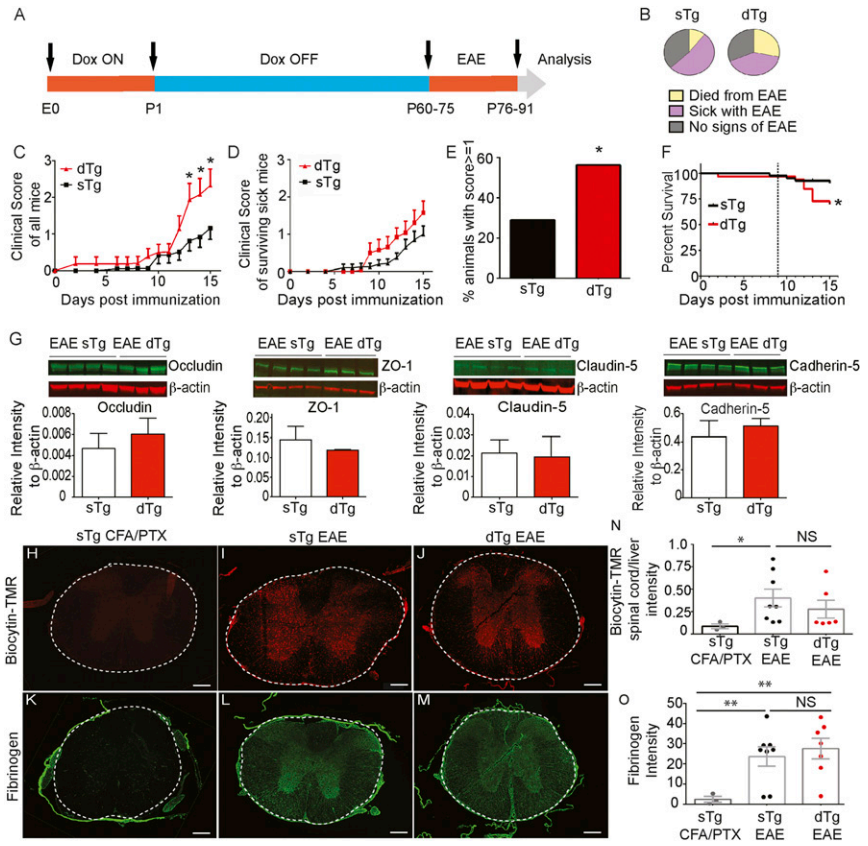

Fig. 5. EC-specific inactivation of the Wnt/β-catenin pathway exacerbates EAE without affecting EC TJs or pathologically increased paracellular BBB permeability. (*A*) Diagram of experimental procedure. (*B*) Pie charts showing the fraction of mice with no signs of EAE (gray) and those that developed clinical EAE (purple) or died from EAE (yellow), in either sTg (TRE-Axin-IRES-eGFP$^{+/-}$ and VE-Cadherin-tTA$^{+/-}$ alone) mice and dTg (VE-Cadherin-tTA$^{+/-}$ TRE-Axin-IRES-eGFP$^{+/-}$) mice. dTg EAE mice died at a higher rate than sTg EAE controls (sTg, $n = 38$; dTg, $n = 32$). (*C* and *D*) Clinical score curves for all (*C*) and surviving (*D*) sTg and dTg mice with EAE. The dTg EAE mice exhibit significantly higher incidence of disease (clinical score ≥1) compared with the sTg EAE mice. sTg, $n = 38$; dTg, $n = 32$. *$P < 0.05$, two-way repeated-measures ANOVA and Sidak's multiple comparison test. (*E*) Graph showing higher incidence of disease induction (score ≥1) for the dTg EAE mice compared with the sTg EAE mice. sTg, $n = 38$; dTg, $n = 32$. *$P < 0.05$, Pearson's χ^2 test. (*F*) Survival curve for the sTg and dTg EAE mice during EAE progression. The dashed line indicates the first day of clinical signs in sTg mice. dTg EAE mice died at a significantly higher rate than sTg EAE controls. sTg, $n = 38$; dTg, $n = 32$. *$P < 0.05$, log-rank Mantel–Cox test. (*G*) Fluorescence Western blotting and quantitation for TJ proteins Occludin, ZO-1, and Claudin-5 plus AJ protein Cadherin-5 for dTg and sTg mice with EAE at similar clinical scores. β-actin served as a loading standard. AJ and TJ protein levels are not significantly different in dTg and sTg EAE mice. (*H–J*) Fluorescence images for biocytin-TMR leakage in thoracic spinal cords of sTg CFA/PTX controls, sTg EAE mice, and dTg EAE mice with similar scores (score 2). (*K–M*) Immunofluorescence images of fibrinogen in thoracic spinal cords for sTg CFA/PTX controls, sTg EAE mice, and dTg EAE mice with similar EAE scores (score 2). (*N*) Graph of biocytin-TMR leakage for sTg CFA/PTX controls ($n = 3$), sTg EAE mice ($n = 8$), and dTg EAE mice ($n = 6$). There is no significant difference in tracer leakage during EAE between the sTg and dTg EAE mice. EAE in sTg mice is significantly more severe than in sTg CFA/PTX controls. *$P < 0.05$, mixed-effects ANOVA. (*O*) Graphs of fibrinogen leakage among sTg CFA/PTX controls ($n = 3$), sTg EAE mice ($n = 8$), and dTg EAE mice ($n = 7$). There is no significant difference in fibrinogen leakage during EAE between sTg and dTg EAE mice, but they both differ significantly from sTg CFA/PTX controls. **$P < 0.01$, mixed-effects ANOVA. Bars represent mean ± SEM. (Scale bars: 200 μm in *H–M*.)

repeated-measures ANOVA and Sidak's multiple-comparison test) (Fig. 5*C*). However, in surviving sick mice, dTg mice exhibited higher (albeit not significantly so) average clinical scores than sTg mice with EAE (Fig. 5*D*). A higher proportion of dTg mice than sTg mice had a clinical score >1.0 (~55%, $n = 32$ vs. ~30%, $n = 38$; *$P < 0.05$, Pearson χ^2 test) (Fig. 5*E*). In addition, dTg mice had a significantly higher death rate compared with sTg mice during the course of EAE (~25% vs. ~5%; *$P < 0.05$, log-rank Mantel–Cox test) (Fig. 5 *B* and *F*).

We examined whether Wnt signaling activation was inhibited in dTg mice compared with sTg mice with EAE. We analyzed *Apcdd1* mRNA expression by in situ hybridization in C57BL/6 CFA/PTX controls as well as C57BL/6 score 3 sTg and dTg EAE score 3 spinal cords. *Apcdd1* mRNA levels were reduced in spinal cords of dTg EAE mice compared with either sTg EAE mice or C57BL/6 score 3 mice, and were similar to those in wild-type CFA/PTX mice (*SI Appendix*, Fig. S7 *A–D*). In addition, the proportion of Sox17$^+$ ECs was lower in dTg mice compared with sTg mice with EAE (15 vs. 35%; *$P < 0.05$, Student's *t* test) (*SI Appendix*, Fig. S7 *E–G*). These results suggest that inhibiting the endothelial Wnt/β-catenin pathway activity during EAE progression significantly worsens the clinical outcomes of the disease.

EC-Specific Inhibition of the Wnt/β-Catenin Pathway Does Not Influence Structural or Functional Paracellular BBB Breakdown During EAE. To assess the effect of EC-specific inhibition of the Wnt/β-catenin pathway on structural and functional BBB properties during EAE, we collected whole spinal cord lysates from sTg and dTg mice at 15 d postinduction for Western blot analysis. We first analyzed the differences between AJ and TJ components that are essential to prevent paracellular movement of blood components into the CNS. Several junctional proteins, including Cadherin-5, β-catenin, Claudin-5, Occludin, and ZO-1, showed no significant differences in the two genotypes undergoing EAE (Fig. 5*G* and *SI Appendix*, Fig. S7*J*). We then administered the low molecular weight tracer 5-(and-6-) tetramethylrhodamine biocytin (biocytin-TMR; 869 Da) i.v. to sTg and dTg mice with similar EAE clinical scores and measured tracer fluorescence intensities in the spinal cord to assess differences in paracellular BBB permeability (24, 63). We found comparable amounts of tracer in the spinal cords from sTg and dTg mice with EAE, whereas the tracer was absent from the CNS tissue of sTg CFA/PTX control mice (Fig. 5 *H–J* and *N*).

We obtained similar results for leakage of plasma fibrinogen across the damaged BBB in sTg and dTg mice with similar EAE scores (Fig. 5 *K–M* and *O*). Therefore, this analysis confirms our finding that AJ and TJ protein levels did not differ between sTg and dTg mice with EAE. Overall, these findings indicate that inhibition of Wnt signaling in ECs during EAE has very little effect on the pathological breakdown of paracellular endothelial barrier regulated by EC junctions.

EC-Specific Inhibition of Wnt/β-Catenin Signaling Promotes Up-Regulation of Immune Cell Adhesion and Transcytosis Proteins in Blood Vessels. The clinical exacerbation of EAE in dTg mice compared with sTg mice, along with their higher death rate (Fig. 5 *B–F*), prompted us to examine the presence and distribution of CD4$^+$ T cells at the peak of the disease (15 d postinduction). At that time,

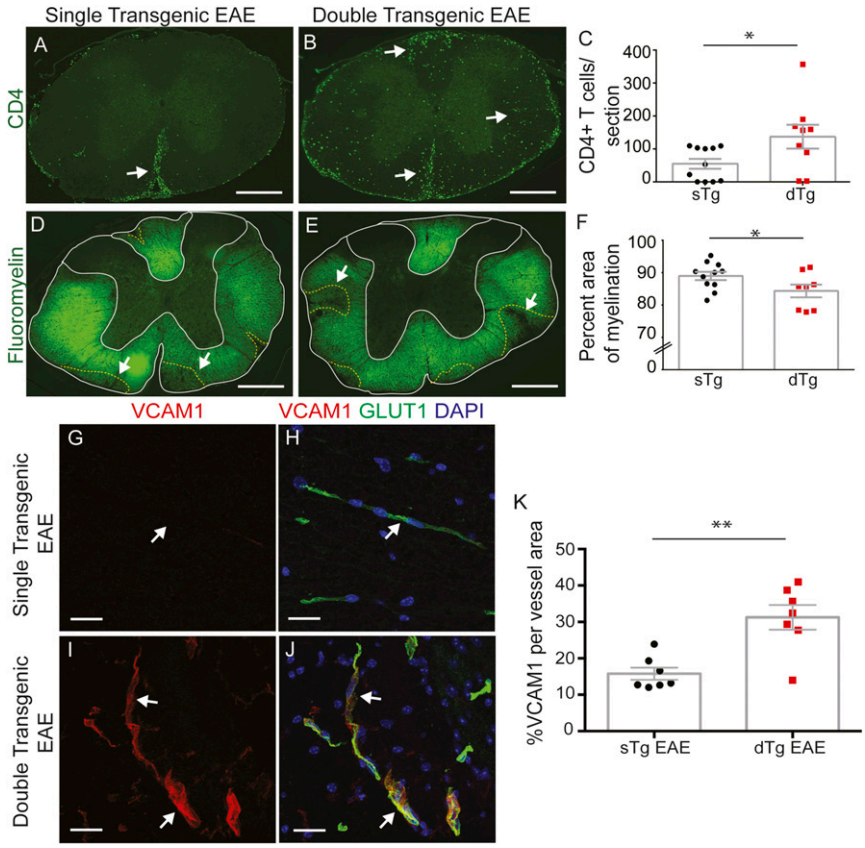

Fig. 6. EC-specific inactivation of the Wnt/β-catenin pathway increases immune cell infiltration into the CNS and demyelination by inducing expression of immune cell adhesion molecules. (*A–C*) Immunofluorescence and quantitation for $CD4^+$ T cells in thoracic spinal cords from sTg and dTg mice with EAE. dTg EAE mice have increased $CD4^+$ T-cell CNS infiltration compared with sTg EAE controls (*A* and *B*, white arrows; *C*, sTg, $n = 11$; dTg, $n = 9$). $^*P < 0.05$, Student's *t* test with unequal variance. (*D–F*) Immunofluorescence for myelin (fluoromyelin) and quantitation of fractional myelinated area in thoracic spinal cords from sTg and dTg mice with similar EAE scores. sTg EAE mice display significantly increased myelination compared with dTg EAE mice (*D* and *E*, white arrows; *F*, sTg, $n = 11$: dTg, $n = 8$). $^*P < 0.05$, Student's *t* test with unequal variance). (*G–L*) Immunofluorescence for VCAM-1 (red), Glut-1 (blood vessel marker; green), and DAPI (nuclei; blue) in sTg and dTg EAE mice at thoracic spinal cord levels. VCAM-1 is highly expressed in blood vessels of dTg EAE mice (*I* and *J*, white arrows). (*K*) Fraction of $VCAM\text{-}1^+$ blood vessels in thoracic spinal cords of sTg and dTg EAE mice. VCAM-1 is significantly elevated in dTg mice during EAE. sTg, $n = 7$; dTg, $n = 7$. $^{**}P < 0.01$, Student's *t* test with unequal variance. Bar graphs represent mean ± SEM. (Scale bars: 200 μm in *A*, *B*, *D*, and *E*; 20 μm in *G–J*.)

$CD4^+$ T cells were three times more abundant on average at both the thoracic and lumbar spinal cord levels in dTg mice compared with sTg mice with EAE (Fig. 6 *A–C* and *SI Appendix*, Fig. S8 *A–C*). We also assessed the extent of demyelination in sTg and dTg EAE mice by fluoromyelin staining. dTg mice had a lower percentage of myelinated area within the spinal cord white matter compared with sTg littermates undergoing active EAE, which was more pronounced in lumbar regions with a more severe pathology ($^*P < 0.05$, unpaired two-tailed *t* test) (Fig. 6 *D–F* and *SI Appendix*, Fig. S8 *D–F*). Therefore, both infiltration of $CD4^+$ T cells in the spinal cord and demyelination are more extensive in dTg mice compared with sTg mice with EAE at 15 d postinduction.

Because canonical Wnt signaling suppresses VCAM-1 in bone marrow stromal and hematopoietic cells (64, 65), we tested whether the increased infiltration of $CD4^+$ T cells in dTg mice with EAE could be due to derepression of VCAM-1 in ECs. We performed immunostaining for VCAM-1 and ICAM-1 in thoracic and lumbar spinal cords of sTg and dTg EAE mice, and quantified the proportions of $VCAM\text{-}1^+$ and $ICAM\text{-}1^+$ vessels. dTg EAE mice showed a ∼1.8- to 2.0-fold increase in the proportion of $VCAM\text{-}1^+$ blood vessels compared with sTg EAE mice (Fig. 6 *G–K* and *SI Appendix*, Fig. S8 *G–K*), whereas ICAM-1 levels were unchanged (*SI Appendix*, Fig. S9).

Finally, we measured the levels of caveolar proteins, which regulate transcellular BBB leakage and provide a route for migrating myelin-specific T cells into the CNS (66) via endothelial caveolae (67–70). We compared Cav-1 and Cavin-2 levels between sTg and dTg EAE mice using quantitative Western blot analysis (LI-COR), and found a ∼50% increase in Cav-1 levels (Fig. 7 *A* and *B*). We then measured the leakage of albumin-Alexa594, a 66-kDa protein that can undergo caveolar transcytosis, in sTg and dTg EAE mice at day 15 postinduction. We used confocal microscopy to assess endothelial-associated albumin (representative of endocytosis) as well as parenchymal-associated albumin, as described previously (24). We found that endothelial-associated albumin was significantly increased in dTg EAE mice compared with sTg EAE mice in lumbar spinal cords (Fig. 7 *C–H* and *SI Appendix*, Fig. S10). These results are consistent with a role for Wnt signaling in suppressing transcellular BBB permeability (32–34). Overall, our findings suggest that counteracting Wnt activation in ECs during EAE increases VCAM-1 and Cav-1 expression to promote both adhesion of $CD4^+$ T cells to blood vessels and their migration into the CNS.

Discussion

A Role for Endothelial Wnt/β-Catenin Pathway in EAE/MS Pathology. It is now well established that robust but transient activation of the Wnt/β-catenin pathway in CNS blood vessels is essential for BBB formation (32–34). Although Wnt/β-catenin signaling activity declines in mature CNS vessels, it is essential for maintaining

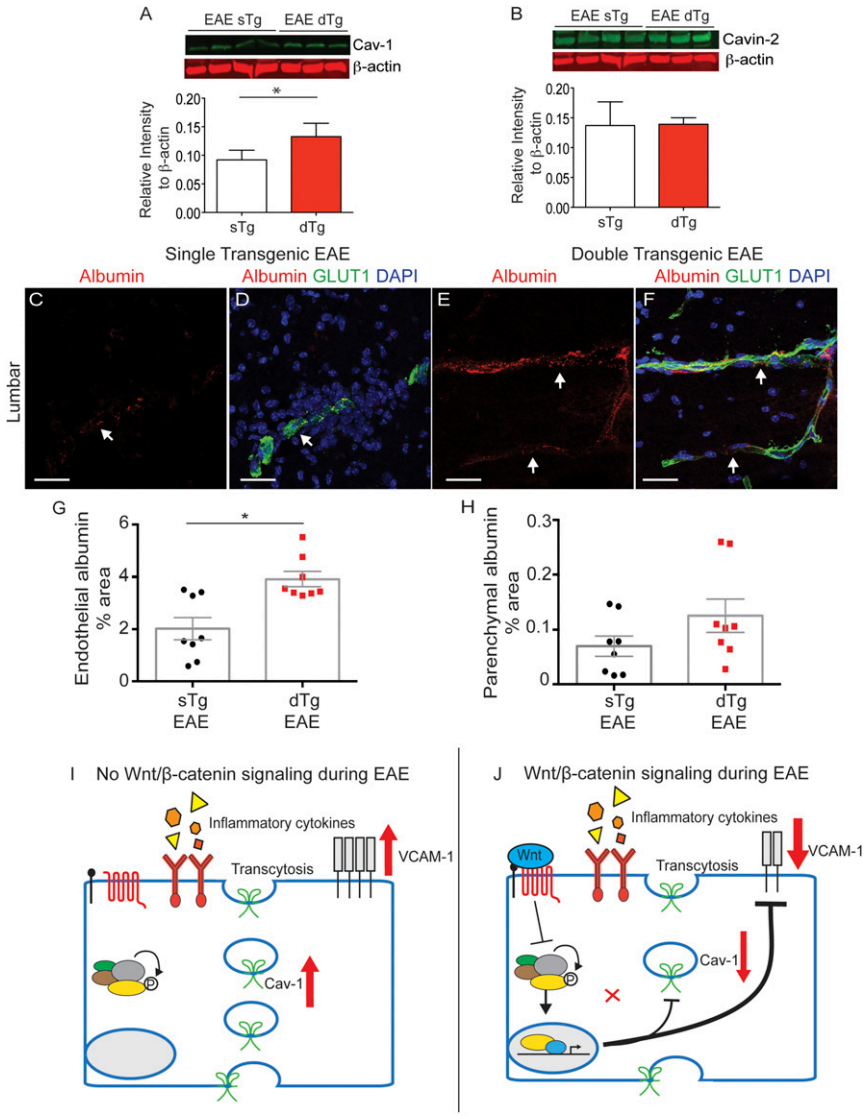

Fig. 7. EC-specific inactivation of the Wnt/β-catenin pathway increases expression of Cav-1 and endothelial endocytosis. (*A* and *B*) Fluorescence Western blots and quantitation for Cav-1 and Cavin-2 transcytosis regulators, with β-actin as a loading control. Cav-1 is significantly higher in dTg EAE mice compared with sTg EAE mice, whereas Cavin-2 levels are similar in the two strains. sTg, $n = 4$; dTg, $n = 3$. *$P < 0.05$; Student's *t* test with unequal variance. (*C*–*F*) BBB leakage of i.v.-infused albumin-Alexa594 (red) in lumbar spinal cord sections from sTg (*C* and *D*) and dTg (*E* and *F*) mice with EAE at day 15 postimmunization. The vascular marker Glut-1 (green) labels endothelial cells, and DAPI (blue) shows nuclei. (*G* and *H*) Bar graphs of the fraction of endothelium-associated or parenchyma-associated albumin traversing the BBB in the lumbar spinal cord. Each dot represents the mean of multiple fields from a single animal. sTg, $n = 8$; dTg, $n = 8$. Bar graphs show mean ± SEM. *$P < 0.05$, two-sided *t* test. (Scale bars: 20 μm.) (*I* and *J*) Schematic diagram summarizing the roles for Wnt signaling in CNS ECs during EAE/MS. In the absence of Wnt ligands, inflammatory cytokines present in the CNS promote high expression of both Cav-1, which regulates endothelial transcytosis, and VCAM-1, which promotes interaction of immune cells with CNS blood vessels. Activation of Wnt/β-catenin signaling in ECs at the peak of EAE inhibits expression of Cav-1 and VCAM-1, two factors that contribute to reduced infiltration by $CD4^+$ T cells into the CNS.

the adult BBB (35, 71, 72). Here we provide in vivo evidence that the Wnt/β-catenin pathway becomes highly activated in CNS endothelium during both EAE and human MS during the course of disease progression. Activation of Wnt signaling in spinal cord blood vessels during EAE correlates with the expression of two ligands, Wnt-3 and Wnt-5a, in the gray matter of the spinal cord, as well as with the disruption of endothelial cell junctions. Because Wnts have a restricted capacity for diffusion within the tissue (73), we infer that β-catenin transcriptional activity in blood vessels is mediated via a ligand-dependent mechanism originating in the gray matter, as well as a putative ligand-independent mechanism owing to the liberation of β-catenin from damaged endothelial cell junctions in demyelinated white matter, including active MS lesions (74).

Why is Wnt signaling activated in blood vessels during neuroinflammation? We hypothesize that pathway reactivation in the CNS endothelium during EAE/MS either partially protects or restores some barrier properties of blood vessels. Consistent with this hypothesis, mice in which we specifically inhibited Wnt signaling in ECs exhibited more severe clinical EAE with increased mortality, greater infiltration of $CD4^+$ T cells into the CNS and more drastic myelin loss. During development, the Wnt/β-catenin pathway stabilizes endothelial AJs and TJs, decreases transendothelial vesicular trafficking, and induces specific transporters for the delivery of essential nutrients to the CNS (32–34). In contrast to its developmental functions, Wnt activation in CNS blood vessels during EAE progression does not prevent the degradation of endothelial junctional proteins or

reduce the paracellular barrier permeability. However, Wnt signaling reduces Cav-1 expression and endothelial endocytosis (Fig. 7 *I* and *J*), consistent with its function during embryonic development (33). Furthermore, Wnt/β-catenin activity in CNS ECs significantly reduces the expression of VCAM-1 (Fig. 7 *I* and *J*), similarly to its function in hematopoietic and stromal cells at that niche (64, 65).

Transcellular permeability via vesicles enriched in Cav-1 and adhesion molecules (e.g., VCAM-1) has been proposed to mediate the trafficking of both cellular and noncellular blood components across the damaged BBB in neuroinflammation (75). Our findings establish that Wnt/β-catenin pathway activation in CNS ECs during EAE suppresses EC adhesion molecule expression and caveolar transport (Fig. 7), thus recapitulating a subset of the roles of Wnts in barrier maturation. One reason that the activation of Wnt signaling has little effect on AJ and TJs in blood vessels during EAE/MS could be the presence of inflammatory and hypoxic molecules in the CNS (76, 77). Inflammatory cytokines such as TNF-α that are abundant in the EAE/MS environment (78), coupled with secretion of VEGF-A or TYMP from astrocytes (79–81), may drive disintegration of endothelial junctions and block the ability of Wnt signaling to restore junctional proteins within the CNS endothelium.

Is activation of the Wnt/β-catenin pathway a feasible translational target for MS therapies? In human MS lesions, pathway activity is detected not only in CNS ECs (Fig. 4 and *SI Appendix*, Fig. S5), but also in oligodendrocytes (82). The Wnt/β-catenin pathway has pleiotropic roles in oligodendrocyte maturation and myelination (83), and transient expression of TCF4 in oligodendrocytes soon after cell cycle exit promotes their maturation and myelination (43). Likewise, APCDD1 also promotes oligodendrocyte maturation (44). However, because APCDD1 is both a target and an inhibitor of the Wnt pathway (40), it is difficult to discern its promyelinating or antimyelinating roles within the CNS. Wnt/β-catenin activity also regulates adaptive immune responses. Targeted deletion of LRP5/6 in dendritic cells suppresses EAE by inhibiting Th1/Th17 helper T-cell differentiation (47). Moreover, pretreatment with the β-catenin agonist SKL2001 reduces the severity of EAE and $CD4^+$ T-cell infiltration into the CNS (47). This indicates that at an organismal level, the protective effect of the Wnt/β-catenin pathway supersedes any deleterious effect on oligodendrocyte maturation in the $MOG_{35–55}$ EAE model. It remains to be determined whether this also holds true in various forms of MS disease, some of which have shown greater potential for remyelination (84).

Our findings suggest that at least part of a protective effect for pharmacologic activation of the Wnt/β-catenin pathway in the $MOG_{35–55}$ EAE animal model in vivo (47) can be attributed to its action within CNS ECs, to partially restore the function of the damaged BBB (transcellular transport) and reduce immune cell infiltration in the CNS. Therefore, pharmacologic activation of Wnt signaling could be a potential disease-modifying treatment in MS. Because BBB breakdown is a component of many neurologic disorders (3), it may be worthwhile to examine a role for Wnt signaling at the barrier in such diseases.

Materials and Methods

Detailed descriptions of the materials and methods used in this study are provided in *SI Appendix, Materials and Methods*. All experimental procedures were approved by the local Institutional Animal Care and Use Committees and Institutional Review Boards.

Wild-type C57BL/6J, *TCF/LEF*::H2B-eGFP reporter (48), VE-Cadherin::tTA (59), and TRE-Axin-IRES-eGFP (60) strains were purchased from the Jackson Laboratory. Doxycyline was administered to pregnant dams where indicated. EAE was induced in female mice with $MOG_{35–55}$. Clinical signs of EAE were scored as follows: 0, no signs; 1, completely flaccid tail; 2, hind limb paresis; 3, hind limb paralysis; 4, hind limb and forelimb paralysis; 5, moribund (85, 86). Patient tissue specimens (*SI Appendix*, Table S2) were provided by C.S.R. (Albert Einstein College of Medicine; IRB #89–31) and the Human Brain and Spinal Fluid Resource Center, VA West Los Angeles Healthcare Center, which is sponsored by the National Institute of Neurological Disorders and Stroke /National Institute of Mental Health, the National Multiple Sclerosis Society, and the Department of Veterans Affairs (D.A.; IRB #AAAQ7343).

Paraffin-embedded brain tissues were used to assess SOX17 expression. Fluorescence Western blot analysis and quantitation was performed as described in *SI Appendix, Materials and Methods*. PFA-fixed cryosections were immunostained and imaged with an LSM700 confocal microscope as described in *SI Appendix, Materials and Methods*. In situ hybridizations were performed using DIG-labeled riboprobes for mouse Wnt-1, -3, -3a, -4, -5a, -7a, -7b, -9a, and -11b; Norrin; and Apcdd1 and human CLAUDIN-5 and APCDD1 in fresh frozen samples as described in *SI Appendix, Materials and Methods* and Tables S1 and S3. EAE mice received i.v. injections of 1% biocytin-TMR or albumin-Alexa594 (Life Technologies) at 30 min before paraformaldehyde perfusion. Tissues were processed as described in *SI Appendix, Materials and Methods*. Images were uniformly thresholded in Fiji, and areas above the threshold were defined as leaky (24). Statistical analyses are described in *SI Appendix, Materials and Methods*.

ACKNOWLEDGMENTS. J.E.L., S.E.L., J.R.S., and D.A. were supported by funding from the NIH National Heart, Lung, and Blood Institute (Grant R01 HL116995-01), the National Institute of Mental Health (Grant R56 MH109987-01A1), the National Multiple Sclerosis Society (Grant RG4673A1/1), and the Leducq Foundation. S.E.L. received a fellowship from the National Multiple Sclerosis Society (Award FG2035-A-1). D.A. is partially supported by an unrestricted gift from John. F. Castle to the Division of Stroke, Department of Neurology at Columbia University Medical Center. C.D. was supported by funding from the NIH National Institute of Neurological Disorders and Stroke (Grant R25 NS070697). C.M.W. is supported by funding from the California Institute for Regenerative Medicine (Grant TR3-05603) and the National Multiple Sclerosis Society (Grant CA 1058-A-8). C.S.R. was a Wollowick Professor at Albert Einstein and was supported by the National Multiple Sclerosis Society (Grant RG1001-K11). The confocal facility in the Optical Biology Shared Resource at the University of California, Irvine was funded by National Institutes of Health Cancer Center Support Grant CA-62203.

1. McFarland HF, Martin R (2007) Multiple sclerosis: A complicated picture of autoimmunity. *Nat Immunol* 8(9):913–919.
2. Daneman R (2012) The blood-brain barrier in health and disease. *Ann Neurol* 72(5): 648–672.
3. Zhao Z, Nelson AR, Betsholtz C, Zlokovic BV (2015) Establishment and dysfunction of the blood-brain barrier. *Cell* 163(5):1064–1078.
4. Nathoo N, Yong VW, Dunn JF (2014) Understanding disease processes in multiple sclerosis through magnetic resonance imaging studies in animal models. *Neuroimage Clin* 4:743–756.
5. Davalos D, et al. (2012) Fibrinogen-induced perivascular microglial clustering is required for the development of axonal damage in neuroinflammation. *Nat Commun* 3:1227.
6. Kermode AG, et al. (1990) Breakdown of the blood-brain barrier precedes symptoms and other MRI signs of new lesions in multiple sclerosis: Pathogenetic and clinical implications. *Brain* 113(Pt 5):1477–1489.
7. Maggi P, et al. (2014) The formation of inflammatory demyelinated lesions in cerebral white matter. *Ann Neurol* 76(4):594–608.
8. Vos CM, et al. (2005) Blood-brain barrier alterations in both focal and diffuse abnormalities on postmortem MRI in multiple sclerosis. *Neurobiol Dis* 20(3):953–960.
9. Absinta M, et al. (2015) Direct MRI detection of impending plaque development in multiple sclerosis. *Neurology* 2(5):e145.
10. Sormani MP, et al. (2009) Magnetic resonance imaging as a potential surrogate for relapses in multiple sclerosis: A meta-analytic approach. *Ann Neurol* 65(3):268–275.
11. Floris S, et al. (2004) Blood-brain barrier permeability and monocyte infiltration in experimental allergic encephalomyelitis: A quantitative MRI study. *Brain* 127(Pt 3): 616–627.
12. Aube B, et al. (2014) Neutrophils mediate blood-spinal cord barrier disruption in demyelinating neuroinflammatory diseases. *J Immunol* 193(5):2438–2454.
13. Miller DH, et al. (1988) Serial gadolinium-enhanced magnetic resonance imaging in multiple sclerosis. *Brain* 111(Pt 4):927–939.
14. Polman CH, et al. (2011) Diagnostic criteria for multiple sclerosis: 2010 revisions to the McDonald criteria. *Ann Neurol* 69(2):292–302.
15. Grossman RI, et al. (1988) Multiple sclerosis: Serial study of gadolinium-enhanced MR imaging. *Radiology* 169(1):117–122.
16. Morita K, Sasaki H, Furuse M, Tsukita S (1999) Endothelial claudin: Claudin-5/TMVCF constitutes tight junction strands in endothelial cells. *J Cell Biol* 147(1):185–194.
17. Nitta T, et al. (2003) Size-selective loosening of the blood-brain barrier in claudin-5-deficient mice. *J Cell Biol* 161(3):653–660.
18. Mark KS, Davis TP (2002) Cerebral microvascular changes in permeability and tight junctions induced by hypoxia-reoxygenation. *Am J Physiol Heart Circ Physiol* 282(4): H1485–H1494.

19. Nag S (2003) Morphology and molecular properties of cellular components of normal cerebral vessels. *Methods Mol Med* 89:3–36.
20. Hnasko R, Lisanti MP (2003) The biology of caveolae: Lessons from caveolin knockout mice and implications for human disease. *Mol Interv* 3(8):445–464.
21. Drab M, et al. (2001) Loss of caveolae, vascular dysfunction, and pulmonary defects in caveolin-1 gene-disrupted mice. *Science* 293(5539):2449–2452.
22. Schubert W, et al. (2002) Microvascular hyperpermeability in caveolin-1 (–/–) knock-out mice: Treatment with a specific nitric-oxide synthase inhibitor, L-NAME, restores normal microvascular permeability in Cav-1 null mice. *J Biol Chem* 277(42):40091–40098.
23. Predescu D, Vogel SM, Malik AB (2004) Functional and morphological studies of protein transcytosis in continuous endothelia. *Am J Physiol Lung Cell Mol Physiol* 287(5):L895–L901.
24. Knowland D, et al. (2014) Stepwise recruitment of transcellular and paracellular pathways underlies blood-brain barrier breakdown in stroke. *Neuron* 82(3):603–617.
25. Nag S, Venugopalan R, Stewart DJ (2007) Increased caveolin-1 expression precedes decreased expression of occludin and claudin-5 during blood-brain barrier breakdown. *Acta Neuropathol* 114(5):459–469.
26. Steiner O, et al. (2010) Differential roles for endothelial ICAM-1, ICAM-2, and VCAM-1 in shear-resistant T cell arrest, polarization, and directed crawling on blood-brain barrier endothelium. *J Immunol* 185(8):4846–4855.
27. Vajkoczy P, Laschinger M, Engelhardt B (2001) Alpha4-integrin-VCAM-1 binding mediates G protein-independent capture of encephalitogenic T cell blasts to CNS white matter microvessels. *J Clin Invest* 108(4):557–565.
28. Baron JL, Madri JA, Ruddle NH, Hashim G, Janeway CA, Jr (1993) Surface expression of alpha 4 integrin by CD4 T cells is required for their entry into brain parenchyma. *J Exp Med* 177(1):57–68.
29. Ifergan I, et al. (2011) Central nervous system recruitment of effector memory $CD8^+$ T lymphocytes during neuroinflammation is dependent on α4 integrin. *Brain* 134(Pt 12): 3560–3577.
30. Yednock TA, et al. (1992) Prevention of experimental autoimmune encephalomyelitis by antibodies against alpha 4 beta 1 integrin. *Nature* 356(6364):63–66.
31. Polman CH, et al.; AFFIRM Investigators (2006) A randomized, placebo-controlled trial of natalizumab for relapsing multiple sclerosis. *N Engl J Med* 354(9):899–910.
32. Daneman R, et al. (2009) Wnt/beta-catenin signaling is required for CNS, but not non-CNS, angiogenesis. *Proc Natl Acad Sci USA* 106(2):641–646.
33. Liebner S, et al. (2008) Wnt/beta-catenin signaling controls development of the blood-brain barrier. *J Cell Biol* 183(3):409–417.
34. Stenman JM, et al. (2008) Canonical Wnt signaling regulates organ-specific assembly and differentiation of CNS vasculature. *Science* 322(5905):1247–1250.
35. Tran KA, et al. (2016) Endothelial β-catenin signaling is required for maintaining adult blood-brain barrier integrity and central nervous system homeostasis. *Circulation* 133(2):177–186.
36. Padden M, et al. (2007) Differences in expression of junctional adhesion molecule-A and beta-catenin in multiple sclerosis brain tissue: Increasing evidence for the role of tight junction pathology. *Acta Neuropathol* 113(2):177–186.
37. Kam Y, Quaranta V (2009) Cadherin-bound beta-catenin feeds into the Wnt pathway upon adherens junctions dissociation: Evidence for an intersection between beta-catenin pools. *PLoS One* 4(2):e4580.
38. Lock C, et al. (2002) Gene-microarray analysis of multiple sclerosis lesions yields new targets validated in autoimmune encephalomyelitis. *Nat Med* 8(5):500–508.
39. Yuan S, Shi Y, Tang SJ (2012) Wnt signaling in the pathogenesis of multiple sclerosis-associated chronic pain. *J Neuroimmune Pharmacol* 7(4):904–913.
40. Shimomura Y, et al. (2010) APCDD1 is a novel Wnt inhibitor mutated in hereditary hypotrichosis simplex. *Nature* 464(7291):1043–1047.
41. Takahashi M, et al. (2002) Isolation of a novel human gene, APCDD1, as a direct target of the beta-catenin/T-cell factor 4 complex with probable involvement in colorectal carcinogenesis. *Cancer Res* 62(20):5651–5656.
42. Fancy SP, et al. (2009) Dysregulation of the Wnt pathway inhibits timely myelination and remyelination in the mammalian CNS. *Genes Dev* 23(13):1571–1585.
43. Hammond E, et al. (2015) The Wnt effector transcription factor 7-like 2 positively regulates oligodendrocyte differentiation in a manner independent of Wnt/β-catenin signaling. *J Neurosci* 35(12):5007–5022.
44. Lee HK, et al. (2015) Apcdd1 stimulates oligodendrocyte differentiation after white matter injury. *Glia* 63(10):1840–1849.
45. Lürbke A, et al. (2013) Limited TCF7L2 expression in MS lesions. *PLoS One* 8(8):e72822.
46. Azim K, Butt AM (2011) GSK3β negatively regulates oligodendrocyte differentiation and myelination in vivo. *Glia* 59(4):540–553.
47. Suryawanshi A, et al. (2015) Canonical wnt signaling in dendritic cells regulates Th1/Th17 responses and suppresses autoimmune neuroinflammation. *J Immunol* 194(7): 3295–3304.
48. Ferrer-Vaquer A, et al. (2010) A sensitive and bright single-cell resolution live imaging reporter of Wnt/ß-catenin signaling in the mouse. *BMC Dev Biol* 10:121.
49. Stromnes IM, Goverman JM (2006) Active induction of experimental allergic encephalomyelitis. *Nat Protoc* 1(4):1810–1819.
50. Corada M, et al. (2013) Sox17 is indispensable for acquisition and maintenance of arterial identity. *Nat Commun* 4:2609.
51. Daneman R, et al. (2010) The mouse blood-brain barrier transcriptome: A new resource for understanding the development and function of brain endothelial cells. *PLoS One* 5(10):e13741.
52. Dejana E (2010) The role of wnt signaling in physiological and pathological angiogenesis. *Circ Res* 107(8):943–952.
53. He X, et al. (1997) A member of the Frizzled protein family mediating axis induction by Wnt-5A. *Science* 275(5306):1652–1654.
54. Valenta T, Hausmann G, Basler K (2012) The many faces and functions of β-catenin. *EMBO J* 31(12):2714–2736.
55. Maretzky T, et al. (2005) ADAM10 mediates E-cadherin shedding and regulates epithelial cell-cell adhesion, migration, and beta-catenin translocation. *Proc Natl Acad Sci USA* 102(26):9182–9187.
56. Reiss K, et al. (2005) ADAM10 cleavage of N-cadherin and regulation of cell-cell adhesion and beta-catenin nuclear signalling. *EMBO J* 24(4):742–752.
57. Kwon EE, Prineas JW (1994) Blood-brain barrier abnormalities in longstanding multiple sclerosis lesions: An immunohistochemical study. *J Neuropathol Exp Neurol* 53(6):625–636.
58. Bennett J, et al. (2010) Blood-brain barrier disruption and enhanced vascular permeability in the multiple sclerosis model EAE. *J Neuroimmunol* 229(1-2):180–191.
59. Sun JF, et al. (2005) Microvascular patterning is controlled by fine-tuning the Akt signal. *Proc Natl Acad Sci USA* 102(1):128–133.
60. Hsu W, Shakya R, Costantini F (2001) Impaired mammary gland and lymphoid development caused by inducible expression of Axin in transgenic mice. *J Cell Biol* 155(6):1055–1064.
61. Brundula V, Rewcastle NB, Metz LM, Bernard CC, Yong VW (2002) Targeting leukocyte MMPs and transmigration: Minocycline as a potential therapy for multiple sclerosis. *Brain* 125(Pt 6):1297–1308.
62. Nikodemova M, Lee J, Fabry Z, Duncan ID (2010) Minocycline attenuates experimental autoimmune encephalomyelitis in rats by reducing T cell infiltration into the spinal cord. *J Neuroimmunol* 219(1-2):33–37.
63. Dileepan T, et al. (2016) Group A *Streptococcus* intranasal infection promotes CNS infiltration by streptococcal-specific Th17 cells. *J Clin Invest* 126(1):303–317.
64. Malhotra S, Kincade PW (2009) Canonical Wnt pathway signaling suppresses VCAM-1 expression by marrow stromal and hematopoietic cells. *Exp Hematol* 37(1):19–30.
65. Ichii M, Frank MB, Iozzo RV, Kincade PW (2012) The canonical Wnt pathway shapes niches supportive of hematopoietic stem/progenitor cells. *Blood* 119(7):1683–1692.
66. Raine CS, Cannella B, Duijvestijn AM, Cross AH (1990) Homing to central nervous system vasculature by antigen-specific lymphocytes, II: Lymphocyte/endothelial cell adhesion during the initial stages of autoimmune demyelination. *Lab Invest* 63(4): 476–489.
67. Carman CV, Springer TA (2004) A transmigratory cup in leukocyte diapedesis both through individual vascular endothelial cells and between them. *J Cell Biol* 167(2): 377–388.
68. Mamdouh Z, Mikhailov A, Muller WA (2009) Transcellular migration of leukocytes is mediated by the endothelial lateral border recycling compartment. *J Exp Med* 206(12):2795–2808.
69. Millán J, et al. (2006) Lymphocyte transcellular migration occurs through recruitment of endothelial ICAM-1 to caveola- and F-actin-rich domains. *Nat Cell Biol* 8(2): 113–123.
70. Wu H, et al. (2016) Caveolin-1 is critical for lymphocyte trafficking into central nervous system during experimental autoimmune encephalomyelitis. *J Neurosci* 36(19): 5193–5199.
71. Wang Y, et al. (2012) Norrin/Frizzled4 signaling in retinal vascular development and blood-brain barrier plasticity. *Cell* 151(6):1332–1344.
72. Zhou Y, et al. (2014) Canonical WNT signaling components in vascular development and barrier formation. *J Clin Invest* 124(9):3825–3846.
73. Farin HF, et al. (2016) Visualization of a short-range Wnt gradient in the intestinal stem-cell niche. *Nature* 530(7590):340–343.
74. Kirk J, Plumb J, Mirakhur M, McQuaid S (2003) Tight junctional abnormality in multiple sclerosis white matter affects all calibres of vessel and is associated with blood-brain barrier leakage and active demyelination. *J Pathol* 201(2):319–327.
75. Carman CV, Springer TA (2008) Trans-cellular migration: Cell-cell contacts get intimate. *Curr Opin Cell Biol* 20(5):533–540.
76. Aboul-Enein F, et al. (2003) Preferential loss of myelin-associated glycoprotein reflects hypoxia-like white matter damage in stroke and inflammatory brain diseases. *J Neuropathol Exp Neurol* 62(1):25–33.
77. Marik C, Felts PA, Bauer J, Lassmann H, Smith KJ (2007) Lesion genesis in a subset of patients with multiple sclerosis: A role for innate immunity? *Brain* 130(Pt 11): 2800–2815.
78. Tigges U, Boroujerdi A, Welser-Alves JV, Milner R (2013) TNF-α promotes cerebral pericyte remodeling in vitro, via a switch from α1 to α2 integrins. *J Neuroinflammation* 10:33.
79. Argaw AT, et al. (2012) Astrocyte-derived VEGF-A drives blood-brain barrier disruption in CNS inflammatory disease. *J Clin Invest* 122(7):2454–2468.
80. Chapouly C, et al. (2015) Astrocytic TYMP and VEGFA drive blood-brain barrier opening in inflammatory central nervous system lesions. *Brain* 138(Pt 6):1548–1567.
81. Wang Y, et al. (2014) Interleukin-1β induces blood-brain barrier disruption by downregulating Sonic hedgehog in astrocytes. *PLoS One* 9(10):e110024.
82. Lee HK, et al. (2015) Daam2-PIP5K is a regulatory pathway for Wnt signaling and therapeutic target for remyelination in the CNS. *Neuron* 85(6):1227–1243.
83. Guo F, et al. (2015) Canonical Wnt signaling in the oligodendroglial lineage—puzzles remain. *Glia* 63(10):1671–1693.
84. Frohman EM, Racke MK, Raine CS (2006) Multiple sclerosis—the plaque and its pathogenesis. *N Engl J Med* 354(9):942–955.
85. Lutz SE, et al. (2013) Contribution of pannexin1 to experimental autoimmune encephalomyelitis. *PLoS One* 8(6):e66657.
86. Lutz SE, Raine CS, Brosnan CF (2012) Loss of astrocyte connexins 43 and 30 does not significantly alter susceptibility or severity of acute experimental autoimmune encephalomyelitis in mice. *J Neuroimmunol* 245(1-2):8–14.